The Effect of Cu and Ge Additions on Strength and Precipitation in a lean 6xxx Aluminium Alloy

The Effect of Cu and Ge Additions on Strength and Precipitation in a lean 6xxx Aluminium Alloy

E A Mørtsell[1, 4], C D Marioara[2], S J Andersen[2], J Røyset[3], O Reiso[3] and R Holmestad[1]

[1]Department of Physics, NTNU, 7491 Trondheim, Norway
[2]SINTEF Materials and Chemistry, N-7465 Trondheim, Norway
[3]Hydro Aluminium R&D Sunndal, N-6600 Sunndalsøra, Norway

E-mail address: eva.mortsell@ntnu.no

Abstract. It has been demonstrated that the strength loss in a lean Al-Mg-Si alloy due to solute reduction could be compensated by back-adding a lower at % of Ge and Cu. Nanosized precipitate needles which are the main cause of strength in these alloys, and material hardness has been correlated to parameters quantified by TEM. It was found that additions of Ge and Cu strongly affect the precipitation process by increasing precipitate density and reducing precipitate size. Investigations of precipitate atomic structure by HAADF-STEM indicated that they contain mixed areas of known phases and disordered regions. A hexagonal Si/Ge-network was found to be present in all precipitate cross sections.

1. Introduction

Aluminium alloys have a vast number of applications, and the 6xxx series in particular is used as extruded and rolled products ranging from car manufacturing to packaging industry. The strength in these age hardenable alloys is caused by the formation of nanosized precipitates shaped like needles growing along the three Al <100> lattice directions [1-9]. The precipitation sequence in ternary Al-Mg-Si alloys is thoroughly characterized and may be given as [1]:

Supersaturated solid solution → atomic clusters → Guinier Preston-zones (pre-*β''*) [2-3] → *β''* [4-5] → *β'* [6], *U1* [7], *U2* [8], *B'* [9] → *β*, Si (stable)

The precipitate needles consist of combinations of the added alloying elements and Al itself, and different precipitate types are found for different alloys and after varying heat treatments. It is essential to find the combinations of solute additions and heat treatment resulting in an optimal balance between strength and production efficiency. Pure aluminium would give the fastest possible extrusion of aluminium alloys [10]. However, the strength of pure aluminium is too low for most applications. In this work, the total amount of Mg and Si in a 6060 Al alloy has been reduced and a lower atomic percentage of Ge and Cu has been back-added. The primary goal of the project has been to maintain initial strength, while increasing extrusion speed because of the lower amount of solutes.

Aberration-corrected High Angle Annular Dark Field Scanning Transmission Electron Microscopy (HAADF-STEM) was chosen as the main characterization technique of the precipitate

[4] To whom any correspondence should be addressed.

atomic structures. Compared to the conventional High Resolution TEM (HRTEM) technique, aberration-corrected HAADF-STEM has several advantages. In addition to a high spatial resolution approaching 0.1 nm, the Z-contrast images are more directly interpretable, being less affected by small changes in objective lens defocus and specimen thickness [11, 12]. With this technique the heavy Ge and Cu atomic columns can be easily identified in the precipitate cross sections.

2. Methods/Materials

An Al 6060 alloy was used as a dense reference, from here on denoted RX0. The second alloy, RXGC1, contained Cu and Ge in addition to the common 6xxx alloying elements. A lean reference, RX1, with reduced Mg and Si contents, directly comparable to RXGC1 in at %, was used as a lean reference alloy. The chemical compositions of the alloys are given in Table 1.

Table 1. Nominal alloy composition in at %. Total effective solute is given in the "total solute"-column.

Alloy	Si	*Ge*	Mg	*Cu*	Fe	*Mn*	*Total Solute*
RX0	0.43	-	0.41	-	0.10	0.015	0.80
RXGC1	0.36	0.02	0.36	0.021	0.10	0.015	0.70
RX1	0.36	-	0.36	-	0.10	0.015	0.66

The alloys were cast, homogenized, extruded and heat treated identical to the description in [13].

TEM investigations have been done for samples artificially aged for 4 hours at 195 °C. Foils for TEM specimens were made by polishing slices from the sample blocks down to a thickness of approximately 100 μm. The foils were electropolished with an electrolyte consisting of one third nitric acid and two thirds methanol kept at -25 °C by adding liquid nitrogen to the solution. The HAADF-STEM images presented in this work were recorded with a double C_s corrected JEOL ARM200F, operated at 200 kV. The probe size was 0.08 nm and the inner collection angle was 50 mrad. For precipitate statistics computed using a methodology described in [14], a Philips CM30 TEM operated at 150 kV and equipped with a Gatan PEELS system was used.

3. Results/Discussions

Statistical results of precipitate microstructure are given in Table 2. It is clear from Table 2 that RXGC1 almost compensates for the strength loss in HV upon removing some Mg and Si. RXGC1 has the same amount of solute as RX1, but the hardness is remarkably higher. This increase in HV can partly be explained by the refinement of microstructure in RXGC1, as compared to RX0. The needles have significantly smaller cross sections and lengths in RXGC1, and in addition the number density has increased by approximately a factor of 50 when comparing to the lean reference RX1. It becomes clear that a lower volume fraction of needles is needed in RXGC1 to achieve approximately the same hardness as for the dense reference RX0.

RX0 does not have any noteworthy amount of disordered precipitates, and β" is the main hardening precipitate. An example of a typical β" cross section in RX0 is shown in Fig. 1 (a), in agreement with [4].

HAADF-STEM revealed RXGC1 to consist of partly disordered precipitates, where the projected hexagonal Si/Ge - network can be observed in all cross sections [10]. Z-contrast confirms a clear trend of Ge replacing or substituting Si network columns, see Fig. 1 (b) and Fig. 2. The strong atomic number dependence of HAADF STEM makes it possible to distinguish Ge (Z = 32) columns and Mg, Al, Si or Cu columns (Z = 12, 13, 14 and 29 respectively). Intensity peaks in the HAADF STEM images correspond directly to atomic column positions.

Table 2. Estimated average precipitate cross sections (CS), needle lengths, number densities, volume fractions and measured Vickers hardness (HV) for each condition. The volume fractions of precipitates are given as 95 % confidence intervals [13]

Alloy	CS [nm^2]	Needle Length [nm]	Number Density [#/μm^{-3}]	Volume Fraction	HV
RX0	24 ± 2	95 ± 5	3200 ± 400	{0.64, 0.80}	77.0
RXGC1	12 ± 1	57 ± 8	8300 ± 1300	{0.48, 0.62}	74.5
RX1	42 ± 4	243 ± 73	170 ± 50	{0.12, 0.19}	50.0

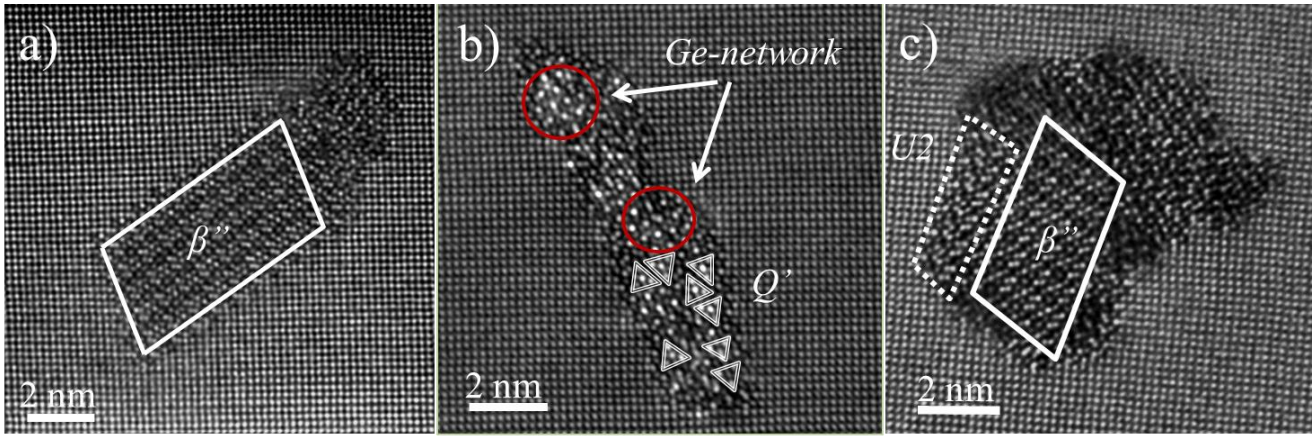

Figure 1. HAADF STEM images of precipitates from the three investigated alloys. The precipitates chosen are typical for the respective alloy and shows that the addition of Ge and Cu strongly affects formation of the phases. The images are taken from a) RX0, b) RXGC1 and c) RX1. In b) the hexagonal Ge-network is indicated with red circles and fragments the Q’ phase are indicated with white triangles. In a) and c) the β” phase is marked with white parallelograms. Part of a U2 phase is also indicated in c) with white dashed lines.

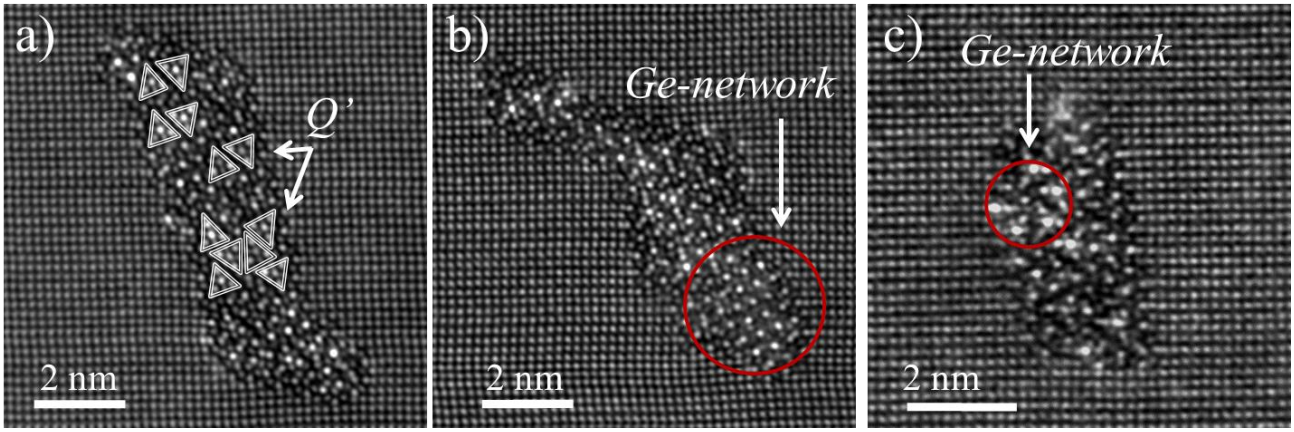

Figure 2. HAADF STEM images of precipitate cross sections from RXGC1. The Ge-network is indicated with arrows and red circles, it is also present in other areas than those pointed out. The Q’ fragments are pointed out with arrows and white triangles. The precipitates in (a) and (b) were found along a dislocation line.

Ge and Cu were found to be present in all precipitate cross sections in RXGC1, so it is clear that these elements play an important role in the precipitation process. Since Ge and Cu are often located also in the centre of the precipitate cross sections it is feasible that they should be active in the nucleation process. As in denser Ge – and Cu containing Al-alloys [15], the Q' phase form frequently also in this leaner alloy (Fig. 2), however, not mixed with the Ge-network.

The cross sections observed in the lean reference alloy RX1 are few and large, see Table 2. An example is given in Fig. 1 (c). The cross sections in this alloy can typically be identified as combinations of several phases. It is usual to find phases associated with overaging of the material here, such as U2 and β'. It should be noted that scan distortions and drift are present in some of the HAADF STEM images. The distortions can in particular be observed in Fig. 2 (b), where the Al lattice has a wave-like appearance in some areas.

4. Conclusions

It has been shown that small additions of Ge in combination with Cu have a strong influence on precipitation in lean 6xxx alloys, leading to high densities of fine precipitates and high hardness values. A lower volume fraction of solute was needed for the Ge- and Cu added alloy in order to obtain the same hardness values as the reference.

The precipitates in the Ge-Cu added alloy were mainly disordered with a hexagonal ordering of Ge/Si columns. Most precipitates also incorporated fragments of the Cu-containing Q' phase. It is clear that Ge and Cu play an important role in the precipitation process.

References

[1] Marioara C D, Nordmark H, Andersen S J, Holmestad R 2006 *J. Mater. Sci.* **41**, pp 471 - 478
[2] Edwards G A, Stiller K, Dunlop G L, Couper M J 1998 *Acta Mater.* **46**, pp 3893 – 3904.
[3] Marioara C D, Andersen S J, Jansen J, Zandbergen H W 2001 *Acta Mater.* **49**, 321-328.
[4] Andersen S J, Zandbergen H W, Jansen J, Træholt C, Tundal U, Reiso O 1998 *Acta Mater.* **46**, pp 3283 – 3298.
[5] Hasting H S, Frøseth A G, Andersen S J, Vissers R, Walmsley J C, Marioara C D, Danoix F, Lefebvre W, Holmestad R 2009 *J. Appl. Phys.* **106**, 123527
[6] Vissers R, van Huis M A, Jansen J, Zandbergen H W, Marioara C D, Andersen S J 2007 *Acta Mater.* **55**, pp 3815 – 3823.
[7] Andersen S J, Marioara C D, Frøseth A, Vissers R, Zandbergen H W 2005 *Mater Sci. Eng.* A **390**, pp 127 – 138.
[8] Vissers R, Marioara C D, Andersen S J, Holmestad R 2008 *Aluminium Alloys* **2**, pp 1263 – 1269.
[9] McLeod D 1962 *Mechanical Properties of Metals* (John Wiley & sons Inc, New York) p 162.
[10] Andersen S J, Marioara C D, Vissers R, Zandbergen H W 2003 *Inst. Phys. Conf. Ser.* **179**, pp 225 – 228.
[11] Nellist P D, Pennycook S J 2000 *Elsevier* **113**, pp. 147 – 203.
[12] Yamazaki T, Kawasaki M, Watanabe K, Hashimoto I, Shiojiri M 2002 *Ultramicroscopy* **92** pp. 181 – 189.
[13] Mørtsell E A, Marioara C D, Andersen S J, Reiso O, Røyset J, Holmestad R 2015 *Met. Trans.* A
[14] Marioara C D, Andersen S J, Zandbergen H W, Holmestad R 2005 *Metall. Mat. Trans.* A, **36**, pp. 691 – 702.
[15] Bjørge R, Marioara C D, Etheridge J 2013 *Imaging and Microscopy*, **4**, pp 39.